Resonance Frequency Spectra with Convergence Tests of Piezoceramic Disks using the Finite Element Method

J. Kocbach

University of Bergen, Department of Physics, Allegaten 55, N-5007 Bergen, Norway

P. Lunde

Christian Michelsen Research AS (CMR), P.O. Box 6031, N-5892 Bergen, Norway

M. Vestrheim

University of Bergen, Department of Physics, Allegaten 55, N-5007 Bergen, Norway

Corresponding author:

J. Kocbach, University of Bergen, Department of Physics, Allegaten 55, N-5007 Bergen, Norway,

tel: (47) 55 58 28 94, fax: (47) 55 58 28 06, E-mail: Jan.Kocbach@fi.uib.no

Shortened title: Resonance Frequency Spectra of Piezoceramic Disks

Summary

Several authors have presented resonance frequency spectra of piezoceramic disks calculated using the Finite Element (FE) method, but the accuracy in these frequency spectra has often not been very high, with relative errors of up to several percent in the calculated resonance frequencies. In the present work, frequency spectra with a maximum relative error of 150 ppm in all calculated resonance frequencies are presented for some of the materials which have been subjected to similar analyses in earlier works; PZT-5A, PZT-5H, $PbTiO_3$, $BaTiO_3$ and $Pb(ZrTi)O_3$. The bound for the relative error is found using an *a priori* error estimator for the calculation of resonance frequencies of piezoceramic disks using the FE method. The error estimator is found based on convergence tests for disks of different piezoceramic materials with varying diameter over thickness ratios. Some work on a corresponding error estimator for electrical and mechanical response functions is also presented.

PACS no. 43.38.Fx, 43.40.Dx, 43.20.Ks, 02.70.D

1. Introduction

Measurement and calculation of resonance frequency spectra of piezoceramic disks (see Fig. 1) have been given considerable attention since the 1950s. One of the most powerful methods for these calculations, is the Finite Element (FE) method. Several authors have presented resonance frequency spectra of piezoceramic disks calculated using the FE method, but the accuracy in these calculations has often not been very high, with relative errors of up to several percent in the calculated resonance frequencies. The purpose of the present work is to present resonance frequency spectra of piezoceramic disks of various materials with improved accuracy and resolution compared to previous work, and to quantify the maximum relative error in the calculated resonance frequencies. A high accuracy in the calculated resonance frequencies is needed in order to present spectra without introducing non-physical effects due to numerical errors. It is also a purpose to compare the characteristics of resonance frequency spectra for disks of different piezoceramic materials.

The focus in the convergence tests is set on the comparison against the ”fully converged FE solution”, and not on comparison against real world results. This is due to the fact that the uncertainties in the material properties provided by the manufactors of piezoelectric materials (see e.g. Ref. [1]) lead to much larger changes in the resonance frequencies than the accuracy which is desired in the present work, thus making it difficult to use measurements for quantitative accuracy considerations. A high accuracy in the calculated resonance frequencies is nevertheless needed in many applications, like for example for accurate determination of material constants of piezoelectric materials and for the calculation of resonance frequency spectra without non-physical effects due to numerical errors. Note, however, that the ”fully converged FE solution” is not obtainable, and that instead a solution with a high number of elements per wavelength, is used as a reference.

When too few elements are used in the FE model of the piezoelectric transducer, the solution may be inaccurate and in some cases even misguiding, but only limited investigations on the accuracy in the FE solution as a function of the element division have been found for FE analysis of piezoelectric structures in the literature. Several different authors have proposed that a certain number of finite elements or finite element nodes should be used per wavelength in the FE model to assure that the solution is found with sufficient accuracy. However, the term sufficient accuracy is not defined, and the proposed number of nodes or elements per wavelength varies from 5-7 finite element nodes per wavelength [2] or 2 quadratic elements per wavelength [3] to 10 linear elements per wavelength [4] or 15 linear elements per wavelength [5]. In the present work, it has been found that when 2 quadratic elements are used per shear wavelength, the relative error (cf. Sec. 4) in the calculated resonance frequencies may be up to 4%, and even less accurate results are to be expected for mechanical and electrical response functions, e.g. mechanical displacement and electrical admittance.

A physical approach to the determination of the number of finite elements needed per wavelength to get a solution which represents the physics of the solution is given for FE analysis of acoustic problems in Ref. [6] - where it is proposed that it is necessary to use 6 linear finite elements per wavelength to get a ”practically useful accuracy”. If quadratic elements are used, a corresponding accuracy can be achieved with less than 6 elements.

Frequency spectra of piezoceramic disks are useful in many applications, including piezoelectric transducer design, because they give information about how the vibrational characteristics of the disks vary with the D/T ratio, and about the degree of coupling between the different vibrational modes. Many papers have been published on both measured and calculated resonance frequency spectra of piezoceramic disks. Often measurements have been compared to analytical solutions for isotropic disks where the piezoelectric effect and anisotropies in the material have been neglected, e.g. in the study of $\mathrm{PbTiO_3}$ disks by Ikegami *et al.* [7], and in studies of $\mathrm{Pb(ZrTi)O_3}$ disks by Ikegami *et al.* [8] and Ueha *et al.* [9]. Shaw's study [10] of $\mathrm{BaTiO_3}$ disks with D/T ratio between 1 and 7 has been compared to both a variational method [11], and the FE method [12, 13, 14] with good qualitative agreement for these low D/T ratios.

Kunkel *et al.* [15, 16] presented frequency spectra of PZT-5H disks with D/T ratio between 0.2 and 10 calculated using the FE method, but according to the authors the calculated resonance frequencies are expected to be about 1.5-2% too high due to the element division used. Investigations have shown that some of the resonance frequencies are more than 3.5% too high [17]. This is not surprising when comparing the finite element mesh used in Ref. [15] with the convergence tests performed in the present work, considering that linear elements were applied, and that only 7 finite element nodes were used per shear wavelength in the radial direction for the highest frequencies presented in Ref. [15].

Guo *et al.* [18, 2] presented frequency spectra of PZT-5A disks calculated using the FE method, but less than 1.5 quadratic elements per shear wavelength were used for the maximum frequency in the thickness direction, yielding inaccurate results. The comparison of Guo's results with a frequency spectrum with better accuracy [13] has shown that the terrace structure around the thickness shear mode is about 9% too high in Ref. [18] due to the coarse element division used in the thickness direction. Furthermore, there are significant differences between results presented in Guo's work and corresponding simulations with identical element divisions and simulation parameters [17] made with the FE codes FEMP [17] ABAQUS [19] and CAPA [20].

Mindlin and Medick [21] have pointed out that the resonance frequency spectra of isotropic disks change significantly, according to whether Poisson's ratio σ is less than, equal to, or larger than the critical value 1/3. Schnabel [22] found that for piezoceramic materials, this corresponds to whether the constant m is less than, equal to, or larger than one, where m is defined by

$$m = f_{r,TE}/f_{r,TS}, \tag{1}$$

and where $f_{r,TE}$ and $f_{r,TS}$ are the resonance frequencies for the fundamental thickness extensional and thickness shear modes in a thin piezoceramic disk, respectively, calculated according to one-dimensional models.

In Refs. [7] and [8] the theory for isotropic disks is compared to experimental results for piezoceramic disks with Poisson's ratio less than and larger than 1/3, respectively, and it is shown that the results for isotropic disks may to some extent be used to understand the vibrational characteristics of piezoceramic disks as well. For an elastic isotropic material with Poisson's ratio less than 1/3 a terrace structure is seen between the frequency minimum and the cut-off frequency for the Lamb mode corresponding to the thickness extensional mode in a calculated frequency spectrum [7]. A corresponding terrace structure is seen in experimental data for the piezoceramic material $\mathrm{PbTiO_3}$ with m less than one. At the cut-off frequency for the thickness shear mode, a weak terrace is seen in both the calculated and measured frequency spectra.

For an elastic, isotropic material with Poisson's ratio larger than 1/3 a corresponding terrace structure is seen between the frequency minimum and the cut-off frequency for the Lamb mode corresponding to the thickness shear mode in a calculated frequency spectrum [8], whereas there is a weak terrace at the cut-off frequency for the thickness extensional mode. This is also the case in the experimental data for the piezoceramic material $\mathrm{Pb(ZrTi)O_3}$ with m larger than one.

In the present work, convergence tests are made for axisymmetric piezoceramic disks with different material properties and with D/T ratios varying from 0.2 to 20. Based on the results from the convergence tests, resonance frequency spectra with maximum relative error in all calculated resonance frequencies of 150 ppm are presented for circular piezoceramic disks. Spectra are presented for some of the materials which have been subjected to similar analyses in previous work; PZT-5A, PZT-5H, $\mathrm{Pb(ZrTi)O_3}$, $\mathrm{BaTiO_3}$ and $\mathrm{PbTiO_3}$. The differences between the resonance frequency spectra are discussed, especially with respect to the value of the constant m. Also presented are frequency spectra of PZT-5A disks with information on electromechanical coupling and average normal displacement over the front of the disk overlayed as circles with varying radius.

The calculations are made using the FE code FEMP [17]. Through comparisons with other FE codes, like ABAQUS [19], CAPA [20] and ANSYS [23], it has been found that FEMP results are equivalent to the results of other FE codes (see Sec. 3), and therefore the current convergence tests and error estimators are considered to be of general interest. The reason for using the FE code FEMP for the calculations is that FEMP is especially well-suited for the systematic analyses in the calculations of the convergence tests and resonance frequency spectra. The theoretical foundation for FEMP is described in Sec. 2.

2. Theory

2.1. The FE formulation

The FE code FEMP is based on a FE formulation for axisymmetric piezoelectric media which has been derived by applying Hamilton's principle to a linear piezoelectric medium, mostly following the works of Allik and Hughes [24], Tiersten [25, 26], and Naillon *et al.* [27]. In the present investigations the effect of a surrounding fluid medium is neglected. A detailed description of the theory is given in Ref. [17]. The resulting FE equations for a piezoelectric medium are the same as the ones given in e.g. Refs. [24, 27, 4, 12, 28]. Below the FE equations for a piezoelectric medium are given on K- and H-form. In addition, the equations used to calculate the resonance frequencies, response functions and coupling coefficient, which are based on the FE equations, are given as a documentation of the method applied.

In a FE process the region of analysis, in this case a piezoceramic disk, is approximated by a finite number of smaller volumes. These volumes are the elements in the FE method. In each element some points, called nodes, are defined where the unknown quantities, in this case mechanical displacement and electrical potential, are to be determined. The relations between the unknown quantities at the nodes of an element and the unknown quantities at an arbitrary point in an element are given by interpolation functions. These interpolation functions are usually polynomials [29]. In most works on piezoelectric FE analysis presented in the literature, either linear or quadratic interpolation functions are applied. In the present work the standard 8 node quadratic isoparametric axisymmetric element with 3×3 Gaussian integration [29] is applied in the analysis for all results presented. Details on this element is given in most textbooks on the FE method (see e.g. Ref. [29]).

Using Hamilton's principle a variational principle is set up for the piezoelectric medium, as described in e.g. Refs [25, 26, 17]. The discretization of this variational principle leads to the FE equations for a piezoelectric medium, where the unknown quantities are the displacement and electrical potential in the nodes of the structure and their derivatives [24],

$$[M_{uu}]\left\{\ddot{\hat{u}}\right\} + [K_{uu}]\{\hat{u}\} + [K_{u\phi}]\left\{\hat{\phi}\right\} = \{F\}, \tag{2}$$

$$[K_{u\phi}]^T\{\hat{u}\} + [K_{\phi\phi}]\left\{\hat{\phi}\right\} = -\{Q\}, \tag{3}$$

where $[M_{uu}]$ is the mass matrix, $[K_{uu}]$ is the mechanical stiffness matrix, $[K_{u\phi}]$ is the piezoelectric stiffness matrix, $[K_{\phi\phi}]$ is the dielectric stiffness matrix, $\{F\}$ is the mechanical force vector, $\{Q\}$ is the electrical charge vector, and $\{\hat{u}\}$ and $\left\{\hat{\phi}\right\}$ are the vectors of displacement and electric potential in the nodes. The symbol $[\;]^T$ denotes the transpose of a matrix, and the dots denote time derivation. Details on the derivation and calculation of the FE matrices for a piezoelectric medium are given e.g. in Refs. [24, 27, 4, 12, 28, 17], and this is therefore not repeated here.

The piezoelectric medium studied in the present work is a circular piezoceramic disk which is polarized in the thickness direction and fully electroded at both major faces. When one electrode is grounded, and the other electrode has potential ϕ (cf. Fig. 1), the FE equations may be rewritten on H-form as [28, 27, 17]

$$[M_{uu}]\left\{\ddot{\hat{u}}\right\} + [H_{uu}]\{\hat{u}\} + \{H_{u\phi}\}\ \phi = \{F\}, \tag{4}$$

$$\{H_{u\phi}\}^T\{\hat{u}\} + H_{\phi\phi}\ \phi = -Q_p, \tag{5}$$

where

$$[H_{uu}] = [K_{uu}] - [K_{u\phi_i}][K_{\phi_i\phi_i}]^{-1}[K_{u\phi_i}]^T, \tag{6}$$

$$\{H_{u\phi}\} = \Big([K_{u\phi_p}] - [K_{u\phi_i}][K_{\phi_i\phi_i}]^{-1}[K_{\phi_i\phi_p}]\Big)[I_p], \tag{7}$$

$$H_{\phi\phi} = [I_p]^T\Big([K_{\phi_p\phi_p}] - [K_{\phi_i\phi_p}]^T[K_{\phi_i\phi_i}]^{-1}[K_{\phi_i\phi_p}]\Big)[I_p], \tag{8}$$

$[I_p]^T = [1\ 1\ 1\ \ldots\ 1]$ is a vector with length equal to the number of nodes on the electrode with varying potential, and Q_p is the charge on the electrode with varying potential ϕ. The matrices $[K_{\phi_p\phi_p}]$ and $[K_{\phi_i\phi_i}]$ are the dielectric stiffness matrices corresponding to nodes which are on the non-grounded electrode and nodes which are on none of the electrodes, respectively. $[K_{u\phi_i}]$, $[K_{u\phi_p}]$ and $[K_{\phi_i\phi_p}]$ are corresponding coupling stiffness matrices.

Resonance frequencies are found by assuming harmonic time dependence, and setting the potential at both electrodes to zero. Thus, the resonance frequencies $\omega_{r,i}$, $i = 1 \ldots 2N$ of a piezoceramic disk are defined by the eigenvalue problem [27, 17]

$$\left([H_{uu}] - \omega_{r,i}^2[M_{uu}]\right)\{\psi_{r,i}\} = 0, \tag{9}$$

where $\{\psi_{r,i}\}$ are the corresponding eigenvectors (or eigenmodes), and N is the number of nodes in the FE model. Losses are neglected in the calculation of the resonance frequencies.

Electrical and mechanical response functions, i.e. electrical input admittance Y and mechanical displacement $[\hat{u}]$, are calculated using the mode superposition method [27, 30, 17]

$$[\hat{u}(\omega)] = \sum_{i=1}^{2N} \frac{-\{\psi_{r,i}\}\{\psi_{r,i}\}^T\{H_{u\phi}\}\phi}{\omega_{r,i}^2 - \omega^2}, \tag{10}$$

$$Y(\omega) = i\omega\Big(\sum_{i=1}^{2N} \frac{\{H_{u\phi}\}^T\{\psi_{r,i}\}\{\psi_{r,i}\}^T\{H_{u\phi}\}}{\omega_{r,i}^2 - \omega^2} - H_{\phi\phi}\Big). \tag{11}$$

The average normal displacement over the front of the disk, $U_{av,z}$, is calculated by

$$U_{av,z} = \frac{1}{A_f}\sum_j \hat{u}_{z,j}\ \Delta A_j, \tag{12}$$

where the sum is over all nodes at the front of the disk. The normal component of displacement at node no. j, which is at the front surface of the disk, is $\hat{u}_{z,i}$, and ΔA_i is the area associated with this node. The total area of the front of the disk is A_f.

An approximate expression for the electromechanical coupling coefficient k_{eff} (sometimes also denoted k_{exp}) is calculated using the mode superposition method, following [31, 27]. k_{eff} is the electromechanical coupling coefficient which may be obtained experimentally by measurement of the characteristic frequencies of the electric impedance of a piezoelectric element by [27]

$$k_{eff}^2 = \frac{\pi}{2}\frac{\omega_{r,i}}{\omega_{a,i}} cot \frac{\pi}{2}\left(\frac{\omega_{r,i}}{\omega_{a,i}}\right) \approx \frac{\omega_{a,i}^2 - \omega_{r,i}^2}{\omega_{a,i}^2}, \tag{13}$$

Here $\omega_{a,i}$ is the antiresonance frequency for mode no. i, defined by the eigenvalue problem [27, 17]

$$\Big\{[H_{uu}] - \{H_{u\phi}\}H_{\phi\phi}^{-1}\{H_{u\phi}\}^T - \omega_{a,i}^2[M_{uu}]\Big\}\{\psi_{a,i}\} = 0, \tag{14}$$

and $\{\psi_{a,i}\}$ are the corresponding eigenmodes. The first expression given for k_{eff} in Eq. (13) is strictly valid only for certain one-dimensional vibrating modes, such as the thickness mode of a disk and the length expander mode of a rod [32], whereas the approximation made in the second part of Eq. (13) is a very good approximation only for intermediate values [27].

By considering Eqs. (9) and (14), an approximate expression of k_{eff} may be found as [27, 31, 17]

$$k_{eff}^2 \approx \frac{k^2(\psi_{r,i})}{1 + k^2(\psi_{r,i})}, \tag{15}$$

where $k(\psi_{r,i})$ is defined by [27, 31, 17]

$$k^2(\psi_{r,i}) = -\frac{\{\psi_{r,i}\}^T\{H_{u\phi}\}H_{\phi\phi}^{-1}\{H_{u\phi}\}^T\{\psi_{r,i}\}}{\{\psi_{r,i}\}^T[H_{uu}]\{\psi_{r,i}\}}. \tag{16}$$

This approximation is based on a perturbation formula [27].

Note that in the expressions for the coupling coefficient, the lossless resonance and antiresonance frequencies are considered.

2.2. Elastic, piezoelectric and dielectric losses

For the calculation of the electrical and mechanical response functions, the losses are included in the eigensolution, making the eigenfrequencies and eigenvectors complex valued. This is done using complex material constants. Thus an imaginary part is added to the elastic stiffness constants at constant electric field c_{pq}^E, the piezoelectric constants e_{ip} and the dielectric constants at constant strain ϵ_{ij}^S, leading to [33, 34],

$$\bar{c}_{pq}^E = c_{pq}^E(1 + i\,\frac{1}{Q_{pq}^{c^E}}), \quad (17)$$

$$\bar{e}_{ip} = e_{ip}(1 + i\,\frac{1}{Q_{ip}^{e}}), \quad (18)$$

$$\bar{\epsilon}_{ij}^S = \epsilon_{ij}^S(1 - i\frac{1}{Q_{ij}^{\epsilon^S}}), \quad (19)$$

where i, j take the values 1, 2, 3 and p, q take the values 1, 2, 3, 4, 5, 6. An overbar denotes a complex valued quantity, and $Q_{pq}^{c^E}$, Q_{ip}^{e} and $Q_{ij}^{\epsilon^S}$ are Q-factors for the elastic stiffness constants, piezoelectric constants and dielectric constants, respectively. In the FE code it is possible to use a full anisotropic set of Q-factors. However, only one mechanical and one electrical loss constant is used in the present work. The value of the mechanical Q-factor Q_m is used for $Q_{pq}^{c^E}$ and $1/\tan\delta_e^T$ is used for $Q_{ij}^{\epsilon^S}$ for all i, j, p and q, on lack of better data. No piezoelectric losses are considered. Material data are given in appendix A1.

2.3. Calculation of the number of elements per wavelength

In the convergence tests presented in the current work, the number of elements per wavelength in the FE model is an important parameter. When the number of elements per wavelength is calculated, it is important to use the appropriate wavelength. The phase velocity of longitudinal and shear waves propagating in piezoceramic disks, and therefore also their wavelengths, differ significantly. The shear wave velocity v_s in a piezoceramic medium is defined by [35]

$$v_s = \sqrt{\frac{c_{44}^E}{\rho}}, \quad (20)$$

where ρ is the density of the piezoceramic, $\lambda_s = v_s/f$ is the wavelength of shear waves, and f is the frequency. The longitudinal wave velocity in the z-direction is defined by [35]

$$v_l = \sqrt{\frac{c_{33}^D}{\rho}}, \quad (21)$$

where c_{pq}^D are elastic stiffness constants at constant electric displacement [36], and $\lambda_l = v_l/f$ is the wavelength of longitudinal waves in the z-direction.

Our investigations have shown that the shortest wavelength, which is the wavelength of shear waves, should be used when the number of elements per wavelength is calculated. This rule is based on a comparison of the number of elements per wavelength needed to get a specified accuracy in radial and thickness direction for several different materials. When the shear wavelength is used, the number of elements per wavelength needed to get a certain accuracy is nearly equal for both radial and thickness direction, and for all materials studied. This is not the case when the wavelength of longitudinal waves is applied.

The number of elements M which must be used to cover a length L with P elements per shear wavelength is given by

$$M = \frac{PL}{\lambda_s} = \frac{PLf}{v_s}, \tag{22}$$

and therefore

$$P = \frac{Mv_s}{Lf}. \tag{23}$$

When a circular piezoceramic disk is modeled using rectangular elements in the rz-plane, a grid of $M_z \times M_r$ elements is used, where M_z is the number of elements used in the thickness direction and M_r is the number of elements used in the radial direction.

2.4. Resonance frequencies for long bars and thin disks

Some resonance frequencies calculated from one-dimensional (1D) analysis of long bars and thin disks are useful in the discussion of the frequency spectra. These are the fundamental resonance frequency $f_{r,LE}$ of a long end-electroded length expander bar with parallel electric field (LE mode), the fundamental resonance frequency $f_{r,TE}$ of a thickness extensional vibrating thin piezoelectric disk (TE mode), and the fundamental resonance frequency $f_{r,TS}$ of a thickness shear vibrating thin piezoelectric disk (TS mode), given by [32, 15]

$$\frac{\pi}{2}\frac{f_{r,LE}}{f_{a,LE}}\cot\left(\frac{\pi}{2}\frac{f_{r,LE}}{f_{a,LE}}\right) = k_{33}^2 \tag{24}$$

$$\frac{\pi}{2}\frac{f_{r,TE}}{f_{a,TE}}\cot\left(\frac{\pi}{2}\frac{f_{r,TE}}{f_{a,TE}}\right) = k_t^2 \tag{25}$$

$$f_{r,TS} = \frac{1}{T}\sqrt{\frac{c_{44}^E}{\rho}} \tag{26}$$

respectively, where $f_{a,LE}$ and $f_{a,TE}$ are the corresponding antiresonance frequencies calculated from 1D analyses [32], defined by

$$f_{a,TE} = \frac{1}{2T}\sqrt{\frac{c_{33}^D}{\rho}} \tag{27}$$

$$f_{a,LE} = \frac{1}{2T\sqrt{\rho s_{33}^D}} \tag{28}$$

The coupling coefficients k_{33} and k_t and the elastic constants s_{33}^D and c_{33}^D are calculated from c_{pq}^E, e_{ip} and ϵ_{ij}^S using formulas given in Ref. [36].

3. Verification of FE results

The focus in the convergence tests is set on comparison against FE simulations in which a high number of elements is used per wavelength. It has therefore been important to check that the FE results are reliable, to ensure that the results given are not in error. A summary of the verification of the FE results is provided here.

Comparisons against measurements, published results and other FE codes have been made. For the comparison against measurements and published results, good qualitative agreement has been achieved in all cases (see e.g. Refs. [17, 37]). For the comparisons against the FE codes ABAQUS [19], ANSYS [23] and CAPA [20], the relative deviation in calculated resonance frequencies compared to these FE codes has been less than 8 ppm for piezoceramic disks with D/T ratio varying from 1 to 20, and for frequencies up to well above the fundamental thickness extensional mode (up to fT = 4000 kHz mm for some D/T ratios) [17]. Details on these comparisons are given in Ref. [17, 37].

In Table I an example of a comparison between resonance frequencies for a PZT-5A disk with D/T ratio equal to 10 calculated with FEMP and ABAQUS is given, to illustrate the good agreement with one of these other FE codes. It is seen from Table I that in this case there is no difference between ABAQUS and FEMP results to the number of decimals delivered by ABAQUS. Thus the deviation between FEMP and ABAQUS results is less than 5 ppm for this case. Due to the good agreement with other, established, FE codes, no comparisons with measurements are shown here. Such comparison are given in Ref. [37].

Note that the resonance frequencies listed are not fully converged to the number of decimals given. That is, when the element division is improved, as in the results presented in Sec. 5, some of the resonance frequencies will shift to a lower value. The resonance frequencies listed may not be too low, because the resonance frequencies converge to the exact value from above [38].

The number of elements per shear wavelength used for each frequency is also given in Table I. Using Fig. 2 it is possible to find the accuracy in each eigenfrequency using the number of elements per shear wavelength, e.g. mode no. 6 is modeled using 9.2 elements per wavelength, leading to a maximum relative error in the resonance frequency of 2×10^{-4}, and the resonance frequency of mode no. 6 may therefore be up to $2 \times 10^{-4} \cdot 1260.99$ kHz $= 0.25$ kHz too high.

4. Convergence tests

A simple method which is often used to check the accuracy in a FE solution is to make two or more simulations of the same problem with different element divisions, and use the difference between these solutions to estimate the accuracy in the solution. Another possible method for finding the accuracy in a FE solution, are various *a posteriori* error estimators based on an energy analysis (see e.g. Refs. [39, 40]). Using this kind of *a posteriori* error estimators, the accuracy in the calculation can be checked when the calculation is completed. If the accuracy is not high enough, a new simulation with improved element division can be made.

The approach chosen in the present work is a systematic extension of the simple method where two or more simulations with different element divisions are compared. However, in the current work more than

1000 simulations of disks of five different piezoceramic materials are done, resulting in an *a priori* error estimator for the calculation of resonance frequencies of piezoceramic disks. The accuracy is given as a function of the number of elements per shear wavelength used in the FE model. Additionally, results for a corresponding error estimator for electrical and mechanical response functions of piezoceramic disks are presented.

The present error estimator is only valid for the 8 node axisymmetric isoparametric element with quadratic variation along the edges [29], which is used for the convergence tests. However, a similar analysis can be made for other element types.

4.1. Convergence tests for resonance frequencies

The error in each calculated resonance frequency is calculated by comparing each calculated resonance frequency with a reference value which is as close to the corresponding fully converged value as possible. In the present work it is chosen to use simulations with 13 elements per shear wavelength, i.e. $P = 13$, for the maximum frequency f_{max} in both radial and thickness direction as reference simulations. Thus, the relative error is computed relative to these reference simulations.

The maximum frequency varies for the different materials considered, but is well above the frequency of the fundamental thickness extensional mode (TE) for all materials. E.g., for PZT-5A disks with thickness 1.0 mm the resonance frequency of the TE mode is $f_{r,TE} = 1935$ kHz. For this case, $P = 13$ for the maximum frequency $f_{max} = 2200$ kHz. This implies that e.g. about 140 elements are used per shear wavelength for $f = 200$ kHz according to Eq. (23) (see Table I for an illustration). Consequently, P for the reference simulations varies from 13 for the maximum frequency to approximately 150 for low frequencies.

The convergence tests are made using six simulation series, where P for the maximum frequency is set to 1.5, 3, 4.5, 6, 7.5 and 9 in both radial and thickness direction, respectively. For each of these cases, all resonance frequencies up to the frequency f_{max} are calculated for disks with 25 different D/T ratios between 0.2 and 20. This is repeated for 5 different materials, PZT-5A, PZT-5H, $\mathrm{Pb(ZrTi)O_3}$, $\mathrm{BaTiO_3}$ and $\mathrm{PbTiO_3}$. Thus about 14000 resonance frequencies are calculated, with P varying from 1.5 to about 100. The relative error in each of these resonance frequencies is calculated relative to the reference simulations.

The relative error as a function of the number of elements per shear wavelength for *each resonance frequency* is plotted as a point in Fig. 2(a). Note that only results for frequencies which are calculated with $P \geq 3$ are shown. When considering a vertical line for $P = 5$ in Fig. 2(a), it may be seen that when 5 elements are used per shear wavelength in both radial and thickness direction in the modeling of a piezoelectric disk, an upper bound for the error is approximately 0.2 %, whereas in some cases much more accurate results may be found, with errors down to 40 ppm. Thus, Fig. 2(a) shows the distribution of the error as a function of the numbers of elements used per shear wavelength. Investigations have shown that these errors are nearly independent of the D/T ratio of the disks, and that the error is lower for some types of vibrational modes than for others [37]. For example, when the same number of elements per shear wavelength is used to model a thickness extensional mode, an edge mode and a thickness shear mode, the error will be lower for the thickness extensional mode than for the edge mode and the thickness shear mode.

In many cases, it is of interest to have an upper bound for the error as a function of the number of elements per shear wavelength. In Fig. 2(b) the maximum relative error as a function of the number of elements per wavelength is plotted for each of the five materials separately. It is seen that the error functions are similar for all five materials. Using this figure, it is straightforward to find which element division should be used to get a certain accuracy. E.g., if a maximum relative error of about 150 ppm is desired, $P = 10$ should be used in both radial and thickness direction. Note that for the reference solution, the number of elements per shear wavelength is 13 for the highest frequencies, and up to 150 for the lowest frequencies. The error is therefore not equal to zero for $P = 13$ in Fig. 2.

When a high number of elements is used in the FE model, it is expected that the numerical error should increase accordingly. In these convergence tests, there have been no indications that this numerical error increases beyond a relative error of 10^{-6}. Furthermore, by comparison with the analytically calculated resonance frequencies of an elastic, isotropic disk using the FE code FEMP, it has been found that when increasing the number of elements per shear wavelength to 200, a relative error of only $2.5 \cdot 10^{-10}$ was found [37], thus indicating that numerical errors are not important in the results shown in the convergence tests in Fig. 2.

Prior to the convergence tests presented in Fig 2, it was investigated if it is appropriate to use the same number of elements per shear wavelength in the radial and in the thickness direction. This was done by calculating the error introduced into the resonance frequencies when P is reduced from 13 to a lower value for f_{max} in each of the coordinate directions separately, while P is held constant at 13 for f_{max} in the other coordinate direction. For each of these two cases, simulations for the same five materials and 25 disks were made. These investigations showed that, for most frequencies, approximately the same number of elements per shear wavelength are needed in radial and thickness direction to get a certain accuracy.

4.2. Convergence tests for mechanical and electrical response functions

Work on a corresponding *a priori* error estimator for electrical and mechanical response functions of piezoceramic disks has been done. When the response functions are calculated using the mode superposition method, more computer memory and computation time is needed than for the resonance frequencies due to the complex valued eigenvalue problem which has to be solved. Therefore, the convergence tests had to be limited to disks with D/T ratio of 5.0 and lower in the present work (10 different D/T ratios between 0.2 and 5.0). Furthermore, the convergence tests are only made for one material, PZT-5A. However, in the convergence tests for the resonance frequencies, it was found that the results were nearly independent of the D/T ratio (not shown here), and that similar results were found for all five materials. This indicates that the *a priori* error estimator developed for electrical and mechanical response functions below may also be applicable to disks with D/T ratio larger than 5.0, and for other piezoceramic materials.

As for the resonance frequencies, six simulation series are made, where P for the maximum frequency f_{max} is set to 1.5, 3, 4.5, 6, 7.5 and 9 in both radial and thickness direction, respectively. Simulations with $P = 13$ for the maximum frequency f_{max} in both radial and thickness direction are again used as reference simulations. The electrical input admittance (Y) and average normal displacement per volt over the front of the piezoceramic disk ($U_{av,z}$) are calculated for frequencies between 200 kHz and 2200 kHz with a frequency step of 2 kHz, for each of the simulation series, including the reference simulations. For each single frequency, P is calculated. Also, the difference between the response functions calculated at this frequency and the reference simulation is calculated, and divided through by the *maximum* value of the response function in the frequency band considered. This error function is used instead of the relative error at the frequency in question, because the response functions are close to zero for some frequencies, and in these cases the relative error therefore becomes very large.

In Fig. 3(a) this error function is plotted as a function of the number of elements per shear wavelength for the input admittance. Corresponding results for the average normal displacement per volt over the front of the disk are presented in Fig. 3(b). For example, from Fig. 3 it is seen that the maximum error is around 5% of the maximum value for the electrical input admittance when $P = 5$. The corresponding maximum error for the average displacement over the front of the disk is 2%.

In Fig. 4 electrical and mechanical response functions for a PZT-5A disk with D/T ratio of 5.0 calculated using $P = 4.5$ for f_{max} in both coordinate directions and the corresponding reference simulations are plotted in the same figure. Results for the electrical input admittance and for the average normal displacement per volt over the front of the disk are shown in Figs. 4(a) and 4(b), respectively. Only minor differences are seen between the case where 4.5 elements are used per shear wavelength in both coordinate directions, and the reference simulations, for both cases. For the enlarged areas, where the error is largest, careful inspection reveals that the differences are mostly due to a slight displacement of the peaks of the electrical input admittance and the average normal displacement towards lower frequencies. This shift of the peaks of the response functions to lower frequencies is the reason for the error in the response functions beeing much larger than the error in the resonance frequencies.

The above results show that the use of 5 elements per shear wavelength seems to give an accuracy for mechanical and electrical response functions which is sufficient for qualitative analysis and in some cases also for comparison with measured values. Convergence tests for electrical and mechanical response functions have only been made for a single piezoceramic material and for D/T ratios of 5.0 and less, but based on the convergence tests for resonance frequencies, where it was found that the results were nearly independent of the D/T ratio and that similar results were found for all five materials, similar results are expected for other materials and D/T ratios for the electrical and mechanical response functions as well.

5. Frequency spectra results

The results of the previous section show that when 10 elements are used per shear wavelength in both thickness and radial direction, the calculated resonance frequencies of piezoceramic disks may be calculated with a maximum relative error of 150 ppm. In the following, frequency spectra for piezoceramic disks are presented with this accuracy using 10 elements per shear wavelength in both radial and thickness direction for the maximum frequency. Note that accordingly most frequencies are calculated with far more than 10 elements per wavelength, and are therefore calculated with far better accuracy than 150 ppm relative error (the accuracy for a specific frequency may be found using Fig. 2).

The resonance frequency spectra show the resonance frequency-thickness product of piezoceramic disks as a function of the D/T ratio of the disks. Frequency spectra are presented in Figs. 5-9 for symmetric modes of disks with D/T ratio between 0.2 and 20 for some materials which have been subjected to similar analyses in previous works (see e.g. Refs. [7, 8, 15, 18, 10]); PZT-5A, PZT-5H, $\mathrm{Pb(ZrTi)O_3}$, $\mathrm{BaTiO_3}$ and $\mathrm{PbTiO_3}$. The thickness of all disks is 1.0 mm. Resonance frequencies have been calculated for 100 different D/T ratios, and results for six D/T ratios for PZT-5A disks are given in appendix A2, as an example. Detailed listings of all resonance frequencies used to plot Figs. 5-9 are given in Ref. [41]. Resonance frequencies for antisymmetric modes have also been calculated, but are not shown here.

The characteristics of the resonance frequency spectra for the different materials are described and compared briefly in this paper. More in-depth analyses of resonance frequency spectra of piezoelectric disks may be found e.g. in Refs. [7, 8, 9, 10, 15, 18, 37].

The theory of Lamb waves in an isotropic plate [15] is useful in the interpretation of the resonance frequency spectra. If only symmetric excitation of an infinite isotropic plate is considered, a spectrum of symmetric dilational plate modes ϕ_1, ϕ_2, ϕ_3, ... will be excited. In a circular disk with a finite diameter, each of these propagating plate modes can give rise to an infinite series of resonance frequency curves, when cross coupling at the circular edges is neglected. At frequencies where only the ϕ_1 plate mode can propagate, only resonances arising from the ϕ_1 mode can exist. These resonances are the radial modes (R modes). When the frequency is increased above the ϕ_2 cutoff frequency, resonances arising from the ϕ_2 propagating mode can exist in the disk, and a new spectrum of resonances, not harmonically related to those below the cutoff frequency, is observed. These modes are classified as anharmonic radial modes (A modes) [7]. For frequencies above the ϕ_3 cutoff frequency, another spectrum of resonances, classified as L modes [9], may be found. In an isotropic, elastic disk with Poissons ratio larger than 1/3, and in a piezoceramic disk with m larger than one [e.g. for PZT-5A, PZT-5H and $\mathrm{Pb(ZrTi)O_3}$], the ϕ_2 plate mode corresponds to the thickness shear mode and the ϕ_3 plate corresponds to the thickness extensional mode. For Poisson's ratio less than 1/3 in an isotropic, elastic disk, and for m less than one in a piezoceramic disk (e.g. for $\mathrm{BaTiO_3}$ and $\mathrm{PbTiO_3}$), the situation is reversed.

5.1. Materials with $m > 1$

Consider the frequency spectrum for circular PZT-5A disks given in Fig. 5. For PZT-5A, m is larger than one. The lowest order mode (mode no. 1 in the figure) approaches the lowest resonance frequency of an end-electroded piezoelectric bar with parallel electric field, the LE mode, as D/T goes to zero. For higher D/T ratios, mode no. 1 is the fundamental radial mode in a piezoceramic disk (R1 in the figure), mode no. 2 is the second radial mode (R2), and so on up to the 10th mode for the highest D/T value shown in the figure. As each of these R modes approaches the region where fT is approximately equal to 1300 kHz mm, the curves representing the modes are flattened, and a weak terrace may be observed in the spectrum. This is the edge mode (E mode) terrace [7, 10, 42], marked with an E in Fig. 5. This terrace does not correspond to a plate mode cutoff frequency. The vibration pattern for modes around this terrace changes to a form having maximum amplitude at the edges of the disk, in contrast to the R modes for which there is little displacement at the edges of the disk.

Going up to higher fT values, a very distinct terrace structure is seen between fT = 1615 kHz mm and fT = 1645 kHz mm. The R modes are disturbed by this terrace structure, but may be connected reasonably well across the terrace. The upper end of the terrace structure is very close to the resonance frequency of the fundamental thickness shear mode in a thin piezoceramic disk, $f_{r,TS}$, which is denoted by TS in Fig. 5. For PZT-5A, $f_{r,TS}$ corresponds to 1650 kHz mm according to Eq. (26). The observation of this terrace structure below the resonance frequency of the TS mode in a thin piezoelectric disk for materials with m larger than one is qualitatively in accordance with theoretical spectra for isotropic disks with Poisson's ratio larger than 1/3, for which a similar terrace structure [8] is observed between the frequency minimum and the cutoff frequency for the ϕ_2 plate mode, which corresponds to the thickness shear mode [15] for isotropic materials with Poisson's ratio larger than 1/3.

With increasing D/T ratio the number of modes in this terrace is increased due to A modes introduced into the spectrum above this terrace [15, 9, 8]. The A modes have a weaker D/T dependence than the R modes for PZT-5A (this is not the case for all materials considered), and may therefore be identified as they cross the R modes above the terrace structure. A detailed identification of the A modes, along with mode shapes for selected D/T ratios, is given in Ref. [37].

The resonance frequency of the fundamental thickness extensional mode in a thin PZT-5A disk, $f_{r,TE}$, is predicted at fT = 1935 kHz mm by Eq. (25). This frequency is marked by TE in Fig. 5. In the resonance frequency spectrum a terrace is seen through a flattening of modes which cross this fT value. This terrace is also in qualitative accordance with the theoretical spectrum for isotropic disks given in Ref. [8], where a similar weak terrace is seen at the cutoff frequency for the ϕ_3 plate mode, which is the thickness extensional mode [15] for isotropic materials with Poisson's ratio larger than 1/3.

Above the frequency $f_{r,TE}$, L modes, which for PZT-5A are strongly coupled with the R modes, may be observed. The L modes are more evident in Fig. 10 due to a higher value for the electromechanical coupling coefficient for the L modes. To the knowledge of the authors, this may be the first time L modes are shown in a frequency spectrum of piezoceramic disks calculated using the FE method.

There is good qualitative agreement between the resonance frequency spectrum for PZT-5A disks presented here, and the corresponding spectrum presented in Refs. [18, 2]. However, due to the high resolution along the D/T axis in the spectrum and high accuracy in the calculated resonance frequencies, the TE mode terrace is seen more clearly in the present work than in Ref. [18, 2]. This improved resolution also makes the identification of L modes and A modes easier. In addition, the terrace structure in the vicinity of the TS mode is predicted at a too high frequency in Ref. [18, 2] due to the poor element division in the thickness direction [13].

The resonance frequency spectra for circular PZT-5H and $\mathrm{Pb(ZrTi)O_3}$ disks, which are both materials with m larger than 1, are shown in Figs. 6 and 7, respectively. The overall characteristics of these resonance frequency spectra are similar to the resonance frequency spectrum for circular PZT-5A disks shown in Fig. 5. The most distinct differences are the frequencies at which the various terraces are observed. For both PZT-5H disks and $\mathrm{Pb(ZrTi)O_3}$ disks, there is good qualitative agreement between the spectra presented here, and corresponding spectra found in the literature [15, 8, 9]. However, the TE mode terrace is seen more clearly in the spectrum for PZT-5H disks in Fig. 6, than in the corresponding spectrum in Ref. [15], due to the higher resolution along the D/T axis and the higher accuracy in calculated resonance frequencies. In addition, the spectra presented in previous works have been calculated for a more limited D/T range.

5.2. Materials with $m < 1$

Resonance frequency spectra of two materials with m less than one, $\mathrm{BaTiO_3}$ and $\mathrm{PbTiO_3}$, are shown in Figs. 8 and 9, respectively. For disks made of these materials, a terrace structure is observed just below the resonance frequency $f_{r,TE}$ of the TE mode in a thin piezoelectric disk, marked with TE in the figures. This terrace structure is similar to the terrace structure found just below the resonance frequency of the TS mode in a thin disk, for materials with m larger than one.

The frequency $f_{r,TE}$ corresponds to fT values of 2569 kHz mm and 2085 kHz mm for $\mathrm{BaTiO_3}$ and $\mathrm{PbTiO_3}$ disks respectively, whereas the terrace structure is observed between fT values of 2420 kHz mm and 2560 kHz mm for $\mathrm{BaTiO_3}$, and between 2000 kHz mm and 2085 kHz mm for $\mathrm{PbTiO_3}$. The observation of this terrace structure below the resonance frequency of the TE mode in a thin piezoelectric disk for materials with m less than one is qualitatively in accordance with theoretical spectra for isotropic disks with Poisson's ratio less than 1/3, where a similar terrace structure [7] is observed between the frequency minimum and the cutoff frequency for the ϕ_2 plate mode, which corresponds to the thickness extensional mode [15] for isotropic materials with Poisson's ratio less than 1/3.

The A modes, which are clearly seen above the terrace structure in Figs. 8 and 9, may easily be identified through their stronger D/T dependence than the R modes. For $\mathrm{PbTiO_3}$, there is very little coupling between R modes and A modes, and therefore the spectral lines corresponding to A modes seem to cross the spectral lines corresponding to R modes almost without perturbation.

For $\mathrm{BaTiO_3}$ and $\mathrm{PbTiO_3}$, the resonance frequency $f_{r,TS}$ is above the resonance frequency $f_{r,TE}$, because m is less than one. Around the resonance frequency $f_{r,TS}$, a weak terrace is observed, analogous to the TE mode terrace for disks with m larger than 1. Above this terrace, the L modes are apparent, especially for $\mathrm{PbTiO_3}$.

For $\mathrm{PbTiO_3}$ disks, there is a very weak coupling between the R modes and the E mode, leading to a very distinct E mode terrace. The R modes are nearly unperturbed by the E mode, and the frequency of the E mode is nearly independent of the diameter for D/T values of about 4 and larger.

For both $\mathrm{BaTiO_3}$ disks and $\mathrm{PbTiO_3}$ disks, there is good qualitative agreement between the spectra presented here, and corresponding spectra found in the literature [10, 43, 7, 12, 14]. However, the spectra for $\mathrm{BaTiO_3}$ disks have only been presented for D/T values between 1 and 7 [10, 43, 12, 14], making the identification of the terraces more difficult.

5.3. Electromechanical coupling coefficient

When using a frequency spectrum in transducer design, it is often important to have information about the vibrational characteristics of the different vibrational modes in the frequency spectrum. Using the FE code, it is easy to plot the eigenmodes corresponding to each resonance frequency and to find mechanical and electrical response functions. It is also possible to calculate an expression for the electromechanical coupling coefficient. By overlaying some of this information on the frequency spectrum, the frequency spectrum may be more valuable for the transducer designer. This is e.g. done in Ref. [15] for the electromechanical coupling coefficient and in Ref. [18] for the modal constant.

In the present work, this type of results are shown for PZT-5A disks, as an example. In these simulations, five elements are used per shear wavelength in both radial and thickness direction for $f_{max} = 2300\ \mathrm{kHz\ mm}$, and the thickness of all disks is 1.0 mm.

In Fig. 10, the frequency spectrum for circular PZT-5A disks is shown, with circles whos radius is proportional to the electromechanical coupling coefficient k_{eff} calculated according to Eq. (15) plotted at each resonance frequency. Note that some circles are too small to be seen. The TE mode is easily identified by the large value for the electromechanical coupling coefficient for fT values around 1935 kHz mm. For D/T ratios of about 7 and smaller, the frequency band with large values for the electromechanical coupling coefficient broadens, and there are typically more than one mode with a large value of k_{eff} for each disk, as also shown in previous work (see e.g. Ref. [15]). The fundamental radial mode has a high value of the electromechanical coupling coefficient, which is nearly independent of the D/T ratio. The E mode terrace is observed to have a higher value of k_{eff} than the R modes in the vicinity of the E mode terrace. The TS terrace structure is observed to have a very low value of the electromechanical coupling coefficient. The A modes above the TS terrace are identified with a lower value of k_{eff} and a weaker D/T dependence than the R modes. The L modes are identified above the TE terrace with a higher value of k_{eff} and a weaker D/T dependence than the R modes.

5.4. Average normal displacement

In Fig. 11 the frequency spectrum for circular PZT-5A disks is shown, with circles whose radius is proportional to the average normal displacement per volt over the front of the disks, $U_{av,z}/V$, plotted at each resonance frequency. The average normal displacement over the front of the disk is calculated using Eq. (12). Note that most circles are too small to be seen on the figure. The terrace around the TE mode is observed to have a large value for $U_{av,z}/V$. The same is seen for the E mode terrace, for low D/T ratios. The fundamental radial mode has the largest value for $U_{av,z}/V$ for all D/T ratios.

6. Conclusions

Convergence tests have been made for axisymmetric piezoceramic disks with different material properties and with D/T ratios varying from 0.2 to 20. The results of the convergence tests have been presented in a diagram which allows the reader to choose an element division which is able to represent all calculated frequencies with a specified accuracy. That is, this diagram may be used as an *a priori* error estimator.

Resonance frequency spectra, with high accuracy in the calculated resonance frequencies, have been presented for several different piezoceramic materials. The accuracy in these resonance frequency spectra is improved compared to previous work. Except for the improvements introduced in the resonance frequency spectra due to better accuracy in the calculated resonance frequencies and better resolution along the D/T axis, the resonance frequency spectra shown in the present work agree well with corresponding resonance frequency spectra presented in previous works, qualitatively.

The improvements in the presented spectra make the analysis and interpretation of the spectra easier than in previous work, and it has therefore been possible to compare frequency spectra for disks of different piezoceramic materials in which no non-physical effects due to numerical errors are visible. The characteristics of these frequency spectra have been compared, especially with respect to the value of the constant m. Spectral lines corresponding to R modes, A modes and L modes have been identified in all resonance frequency spectra, and the position of E mode, TS mode and TE mode terraces and terrace structures have been pointed out. It has also been shown that in resonance frequency spectra where circles with radius equal to the electromechanical coupling coefficient are plotted at each resonance frequency, the mode identification is made easier. This has made it possible to identify three different L modes above the TE mode in the frequency spectrum for PZT-5A disks, due to the fact that the electromechanical coupling coefficient is larger for the L modes than for the R modes in this frequency region.

Acknowledgement

This work has received support from the Research Council of Norway, and from the Norwegian Supercomputing Committee through a grant of computing time. The authors would also like to thank the staff at the Institute of Measurement Technology at the Johannes Kepler University of Linz for the use of the FE programs CAPA and ABAQUS in comparisons with the FE code used in the present work.

Appendix

A1. Material parameters

Material parameters for the five materials used in the present work are given in Table A1. The material parameters for PZT-5A and PZT-5H are taken from Ref. [1], and the material parameters for $\mathrm{BaTiO_3}$ are taken from Ref. [32]. Material parameters for $\mathrm{Pb(ZrTi)O_3}$ and $\mathrm{PbTiO_3}$ are given in Refs. [8] and [44] respectively, using the elastic compliance s^E_{pq} and piezoelectric constants d_{ip} instead of the elastic stiffness constants c^E_{pq} and piezoelectric constants e_{ip} which are used as input for the present FE model. The values of c^E_{pq} and e_{ip} given in Table A1 are calculated from s^E_{pq} and d_{ip} using formulas given in Ref. [36] for $\mathrm{PbTiO_3}$ and $\mathrm{Pb(ZrTi)O_3}$. For all calculations, the number of decimals given in the table is used in the calculations.

For the electrical and mechanical response calculations for PZT-5A disks, the values $Q_m = 75$ and $\tan\delta^T_e = 0.02$ are used for the losses.

A2. Resonance frequencies for PZT-5A disks

Resonance frequencies for six PZT-5A disks with D/T ratio of 1.0, 4.0, 8.0, 12.0, 16.0 and 20.0 calculated using 10 elements per shear wavelength in both coordinate directions for the maximum frequency $f_{max} = 2300\mathrm{kHz\ mm}$, are shown in Table A2. The thickness of all disks is 1.0 mm. These results are presented with 6-digit accuracy as a reference for comparisons for future work, as there are no benchmark values available in the literature for calculated resonance frequencies of piezoelectric disks. Corresponding listings of resonance frequencies for disks of PZT-5A, PZT-5H, $\mathrm{Pb(ZrTi)O_3}$, $\mathrm{BaTiO_3}$, and $\mathrm{PbTiO_3}$ with 100 different D/T ratios between 0.2 and 20 are given in Ref. [41].

References

[1] Five piezoelectric ceramics, Bulletin 66011/F. Vernitron Ltd., England, 1976 (now Morgan Matroc Ltd.).

[2] N. Guo: The vibration characteristics of piezoelectric discs. Dissertation. Department of Mechanical Engineering, Imperial College of Science, Technology and Medicine, London, 1989.

[3] P. Lanceleur, J. Francois de Belleval, N. Mercier: Modeling of transient deformation of piezoelectric ceramics. IEEE Trans. Ultrason. Ferr. Freq. Contr. **39** (1992) 293–301.

[4] H. Jensen: Calculations for piezoelectric ultrasonic transducers Risø National Laboratory, Denmark, 1986.

[5] G. Wojcik, D. Vaughan, N. Abboud, J. Mould Jr.: Electromechanical modeling using explicit time-domain finite elements. Proc. of 1993 IEEE Ultrason. Symp., IEEE, New York, 1993. 1107–1112.

[6] M. Jensen: Acoustic finite element calculations in the time domain. Dissertation. Department of Acoustic Technology, Technical University of Denmark, Denmark, 1996.

[7] S. Ikegami, L. Ueda, S. Kobayashi: Frequency spectra of resonant vibration in disk plates of $\mathrm{PbTiO_3}$ piezoelectric ceramics. J. Acoust. Soc. Am. **55** (1974) 339–344.

[8] S. Ikegami, T. Nagata, Y. Nakajima: Frequency spectra of extensional vibration in $\mathrm{Pb(ZrTi)O_3}$ disks with Poisson's ratio larger than 1/3. J. Acoust. Soc. Am. **60** (1976) 113–116.

[9] S. Ueha, S. Sakuma, E. Mori: Measurement of vibration velocity distributions and mode analysis in thick disks of $\mathrm{Pb(ZrTi)O_3}$. J. Acoust. Soc. Am. **73** (1983) 1842–1847.

[10] E. Shaw: On the resonant vibrations of thick Barium Titanate disks. J. Acoust. Soc. Am. **28** (1956) 38–50.

[11] E. EerNisse: Variational method for electroelastic vibration analysis. IEEE Trans. Son. Ultrason. **SU-14** (1967) 153–160.

[12] R. Lerch: Simulation of piezoelectric devices by two- and three-dimensional finite elements. IEEE Trans. Ultrason. Ferr. Freq. Contr. **37** (1990) 233–247.

[13] J. Kocbach: Finite element modeling of piezoelectric disks. Diploma Thesis. Department of Physics, University of Bergen, Norway, 1996. (in Norwegian).

[14] A. Ishizaki, H. Sekimoto: Two-dimensional analysis using one-dimensional FEM for straight-crested waves in arbitrary anisotropic crystal plates and axisymmetric piezoelectric vibrations in ceramic disks. IEEE Trans. Ultrason. Ferr. Freq. Contr. **43** (1996) 811–817.

[15] H. Kunkel, S. Locke, B. Pikeroen: Finite-element analysis of vibrational modes in piezoelectric ceramic disks. IEEE Trans. Ultrason. Ferr. Freq. Contr. **37** (1990) 316–328.

[16] S. Locke, H. Kunkel, B. Pikeroen: Finite element modeling of piezoelectric ceramic disks. 1987 Ultrason. Symp. Proc., New York, 1987. IEEE, 701–706.

[17] J. Kocbach, P. Lunde, M. Vestrheim: FEMP, Finite Element Modeling of Piezoelectric structures. Theory and verification for piezoelectric disks . Scientific/Technical Report No. 1999-07, Department of Physics, University of Bergen, Norway, 1999.

[18] N. Guo, P. Cawley: The finite element analysis of the vibration characteristics of piezoelectric discs. J. Sound Vib. **159** (1992) 115–138.

[19] Abaqus/Standard Users Manual Version 5.4. Hibbit, Karlsson & Sorensen, USA, 1994.

[20] H. Landes, R. Lerch, M. Kaltenbacher: CAPA Verification-Manual, Release 3 Version 1.0. Institute of Measurement Technology, University of Linz, Linz, Austria, 1998.

[21] R. Mindlin, M. Medick: Extensional vibrations of elastic plates. ASME J. Appl. Mech. **26** (1959) 561–569.

[22] P. Schnabel: Dispersion of thickness vibrations of piezoceramic disk resonators. IEEE Trans. Son. Ultrason. **SU-25** (1978) 16–24.

[23] Ansys revision 5.0. Technical description of capabilities. Swanson Analysis Systems, Inc., PA, USA, 1992.

[24] H. Allik, T. Hughes: Finite element method for piezoelectric vibration. Int. J. Num. Meth. Eng. **2** (1970) 151–157.

[25] H. Tiersten: Natural boundary and initial conditions from a modification of Hamilton's principle. J. Math. Phys. **9** (1968) 1445–1451.

[26] H. Tiersten: Linear piezoelectric plate vibrations: Elements of the linear theory of piezoelectricity and the vibrations of piezoelectric plates. Plenum Press, New York, 1969.

[27] M. Naillon, R. Coursant, F. Besnier: Analysis of piezoelectric structures by a finite element method. Acta Electr. **25** (1983) 341–362.

[28] D. Boucher, M. Lagier, C. Maerfeld: Computation of the vibrational modes for piezoelectric array transducers using a mixed finite element-pertubation method. IEEE Trans. Son. Ultrason. **SU-28** (1981) 318–330.

[29] O. Zienkiewicz: The finite element method. McGraw-Hill, New York, 1977.

[30] H. Bathe: Finite element procedures in engineering analysis. Prentice-Hall, Inc., New Jersey, 1982.

[31] M. Naillon, F. Besnier, R. Coursant: Finite element analysis of narrow piezoelectric parallepiped vibrations. Energetical coupling modeling. 1983 IEEE Ultrason. Symp. Proc., Atlanta, 1983. 773–777.

[32] D. Berlincourt, D. Curran, H. Jaffe: Piezoelectric and piezomagnetic materials and their function in transducers. Physical Acoustics, New York, 1964. W. P. Mason (ed.). Academic Press, 170–269.

[33] T. Ikeda: Fundamentals of piezoelectricity. Oxford University Press, Oxford, UK, 1990.

[34] R. Holland, E. EerNisse: Design and analysis of piezoelectric resonant devices. The M.I.T. press, Cambridge, Massachusetts and London, England, 1969.

[35] B. Auld: Acoustic fields and waves in solids: Vol I. Krieger Publishing Company, Malabar, Florida, 1990.

[36] IEEE standard on piezoelectricity - Std. 176 - 1987. The Institute of Electrical and Electronics Engineers, Inc., New York, 1988.

[37] J. Kocbach: Finite element modeling of ultrasonic piezoelectric transducers. Influence of geometry and material parameters on vibration, response functions and radiated field. Dissertation. Department of Physics, University of Bergen, 2000.

[38] R. Cook: Concepts and applications of finite element analysis, 2nd ed. Wiley, New York, 1981.

[39] R. Tetambe, C. Rajakumar: Estimation of error in finite element acoustic analysis. Computers & Structures **61** (1996) 13–19.

[40] C. Zhao, G. Steven: *A Posteriori* error estimator/corrector for natural frequencies of thin plate vibration problems. Computers & Structures **59** (1996) 949–963.

[41] J. Kocbach, P. Lunde, M. Vestrheim: Tables of resonance frequencies for disks of PZT-5A, PZT-5H, $\mathrm{Pb(ZrTi)O_3}$, $\mathrm{BaTiO_3}$ and $\mathrm{PbTiO_3}$. Scientific/Technical Report No. 2000-07, Department of Physics, University of Bergen, Norway, 2000.

[42] D. Gazis, R. Mindlin: Extensional vibrations and waves in a circular disk and a semi-infinite plate. J. Appl. Mech. **27** (1960) 541–547.

[43] R. Holland: Resonant properties of piezoelectric ceramic rectangular parallelepipeds. J. Acoust. Soc. Am. **43** (1968) 988–997.

[44] S. Ikegami, I. Ueda, T. Nagata: Electromechanical properties of $\mathrm{PbTiO_3}$ ceramics containing La and Mn. J. Acoust. Soc. Am. **50** (1971) 1060–1066.

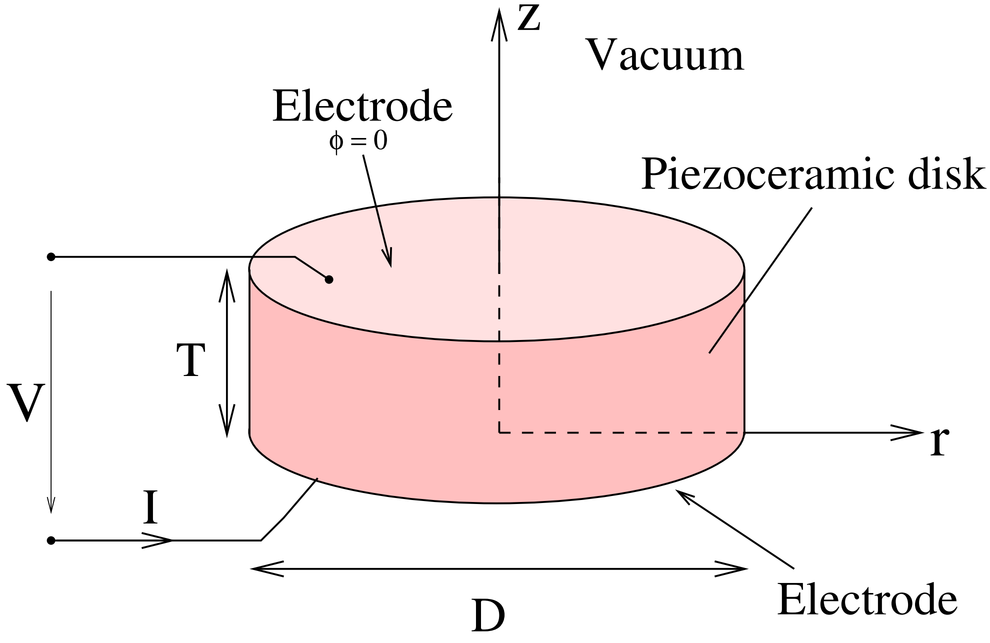

Figure 1. A piezoceramic disk in vacuum with thickness T and diameter D. The upper electrode is grounded.

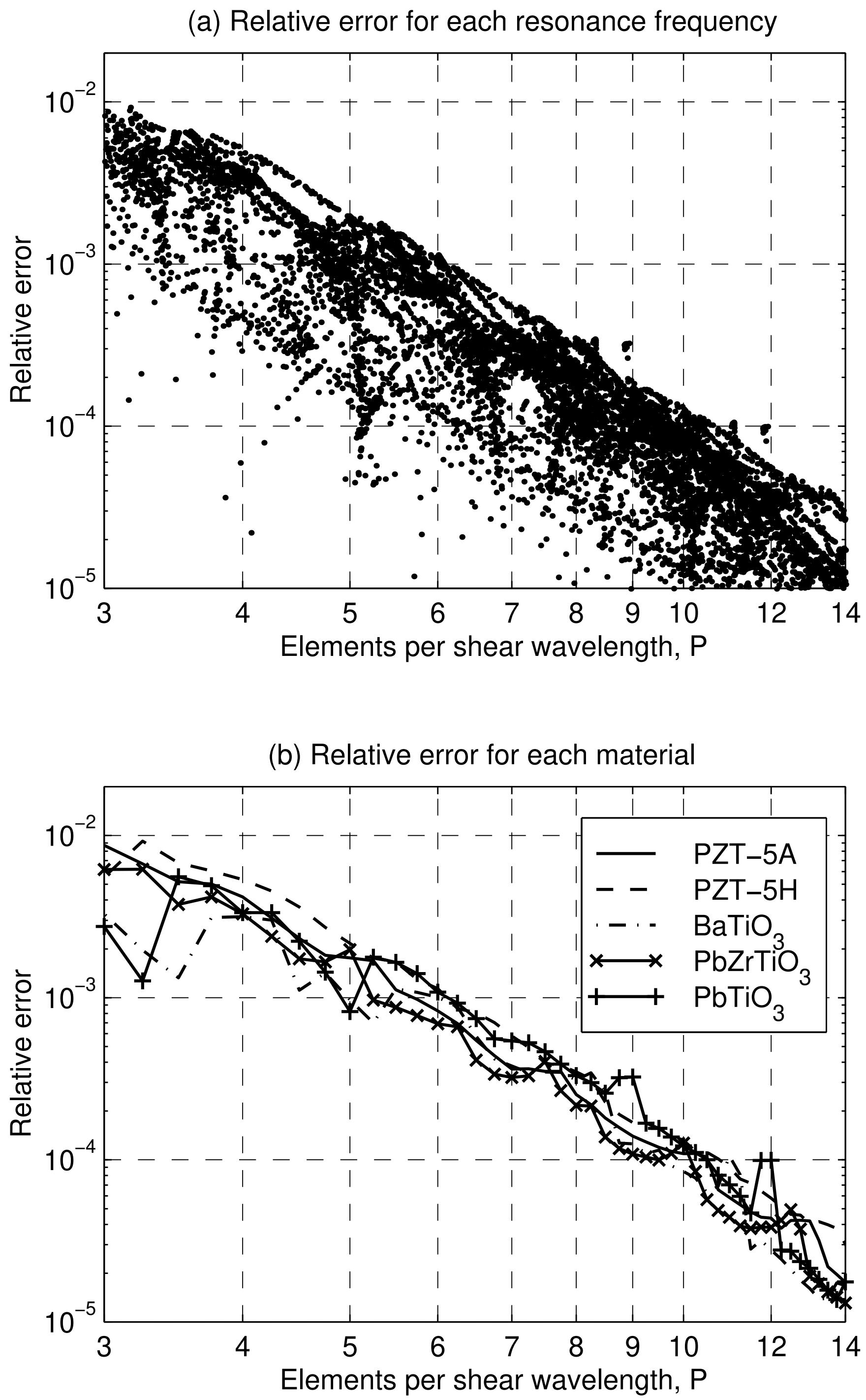

Figure 2. In (a) the relative error in each calculated resonance frequency is plotted as a function of the number of elements per shear wavelength in radial and thickness direction. Resonance frequencies for disks of PZT-5A, PZT-5H, $\mathrm{BaTiO_3}$, $\mathrm{PbTiO_3}$ and $\mathrm{Pb(ZrTi)O_3}$ with D/T ratio between 0.2 and 20 are included, for frequencies up to well above the fundamental thickness extensional mode of the disks. In (b) the maximum relative error for each of the five materials is plotted as a function of the number of elements per shear wavelength (P) used in the FE model.

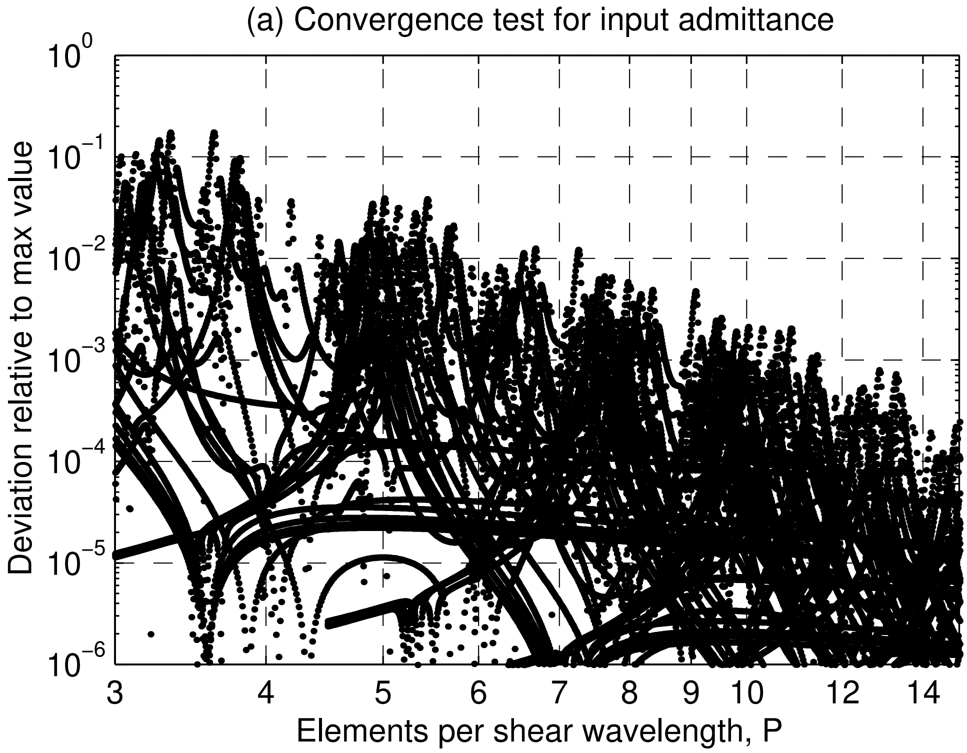

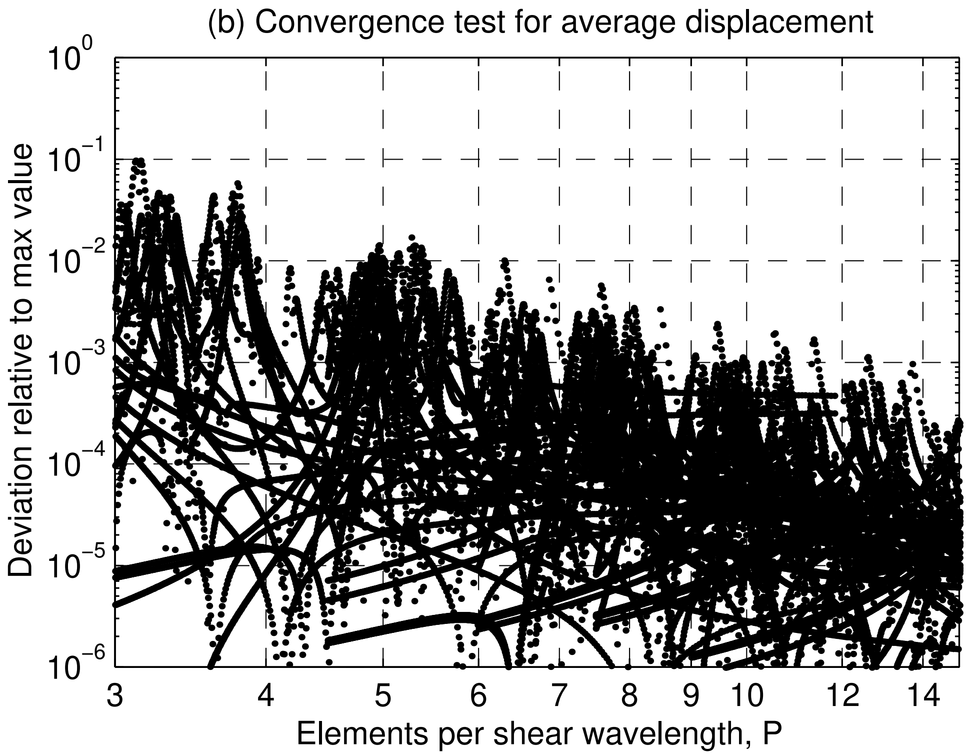

Figure 3. In (a) the relative error in calculated electrical input admittance for 1000 frequencies between 200 kHz and 2200 kHz is plotted as a function of the number of elements per shear wavelength for PZT-5A disks with D/T ratio between 0.2 and 5. In (b) corresponding results for the average normal displacement per volt over the front of the disk is plotted.

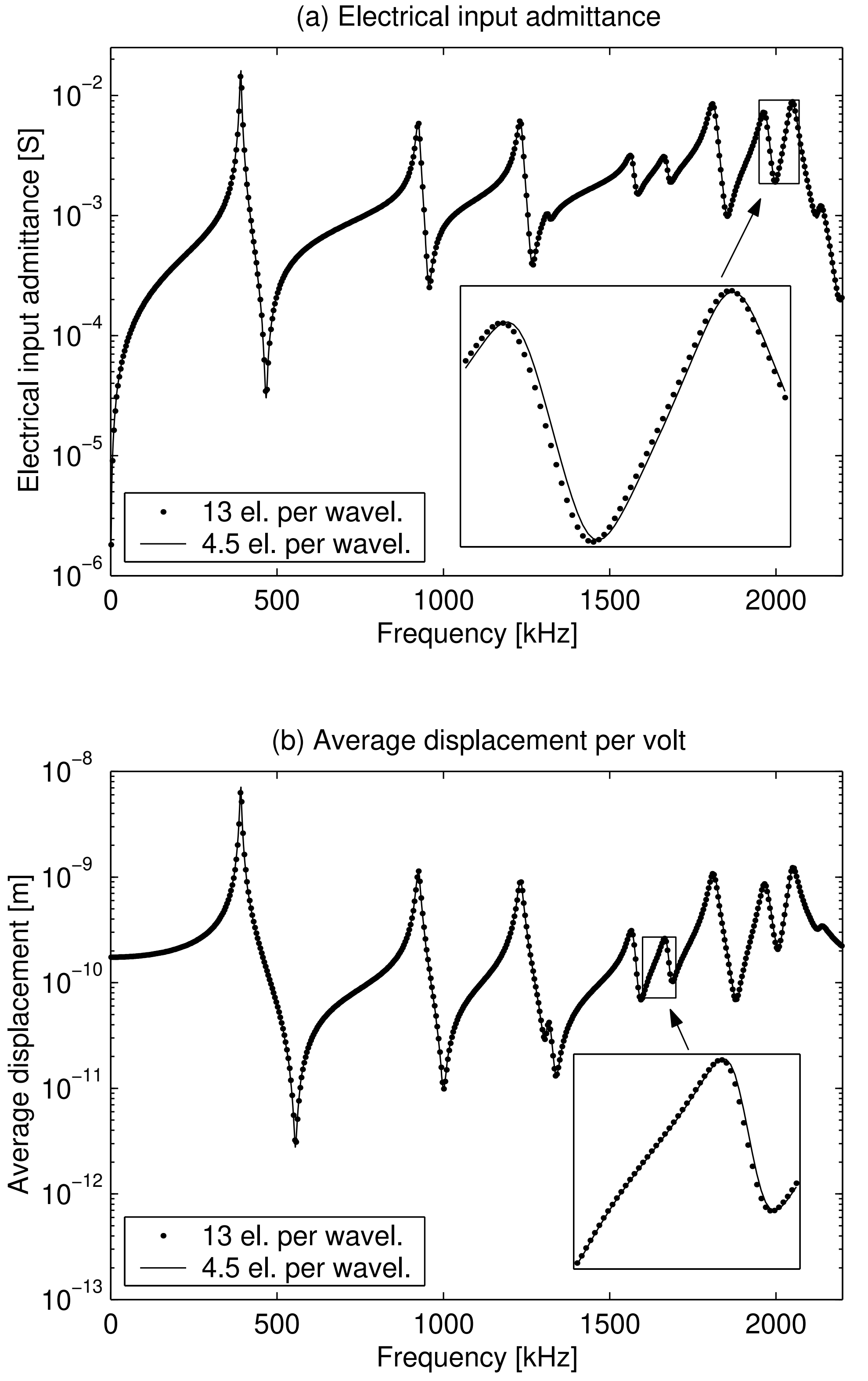

Figure 4. The electrical input admittance and average normal displacement per volt over the front of the disk for a PZT-5A disk with thickness 1.0 mm and diameter 5.0 mm is shown in (a) and (b) respectively. The solid line is for simulations using $P = 4.5$ for $fT = 2200$ kHz. Corresponding simulation results with $P = 13$ for $fT = 2200$ kHz are shown using dots.

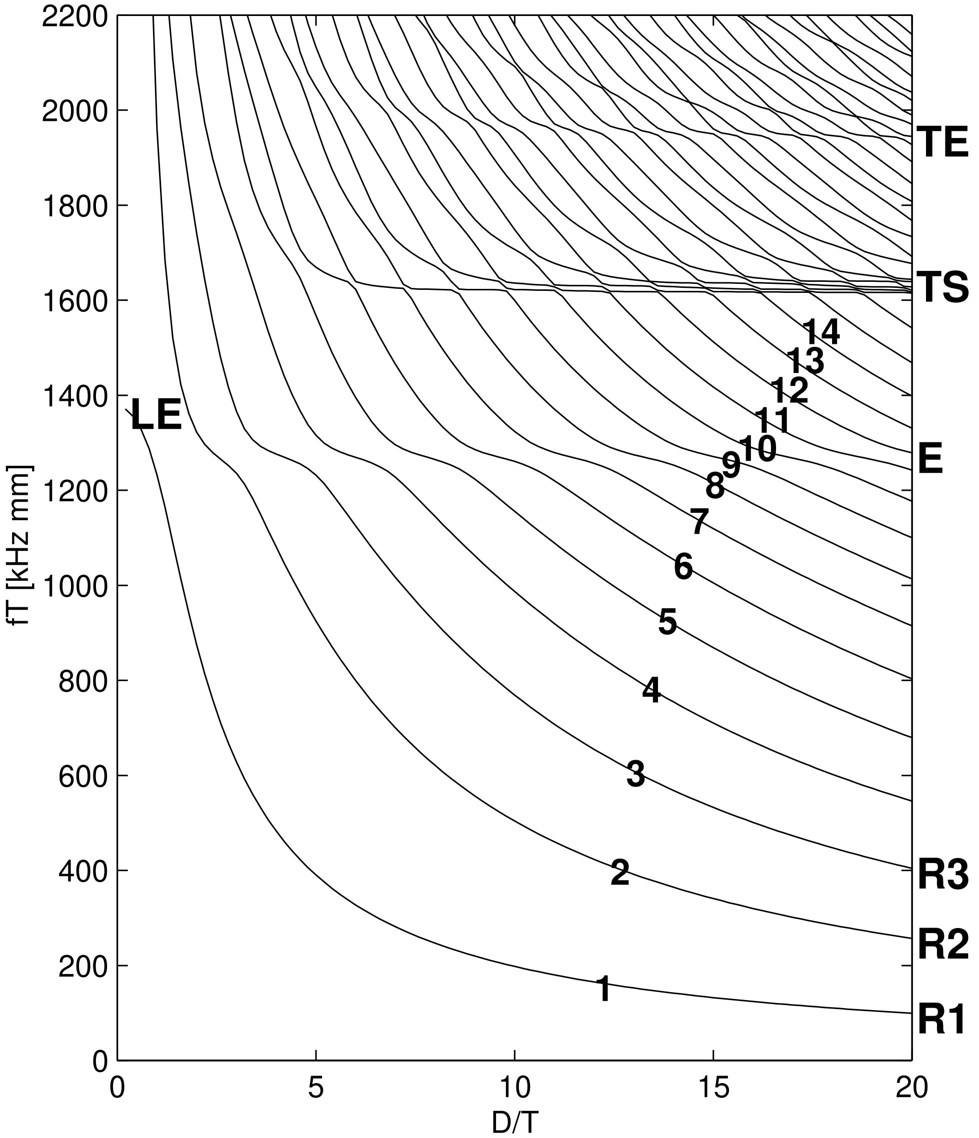

Figure 5. Resonance frequency spectrum for the symmetric modes of circular PZT-5A disks. Mode numbers of the 14 lowest order modes are given using bold numbers. Mode names for the R1 . . . R3 modes are included, and the frequencies $f_{r,LE}$, $f_{r,TS}$ and $f_{r,TE}$ are identified by the symbols LE, TS and TE, respectively. In addition, the E mode terrace is identified using the symbol E.

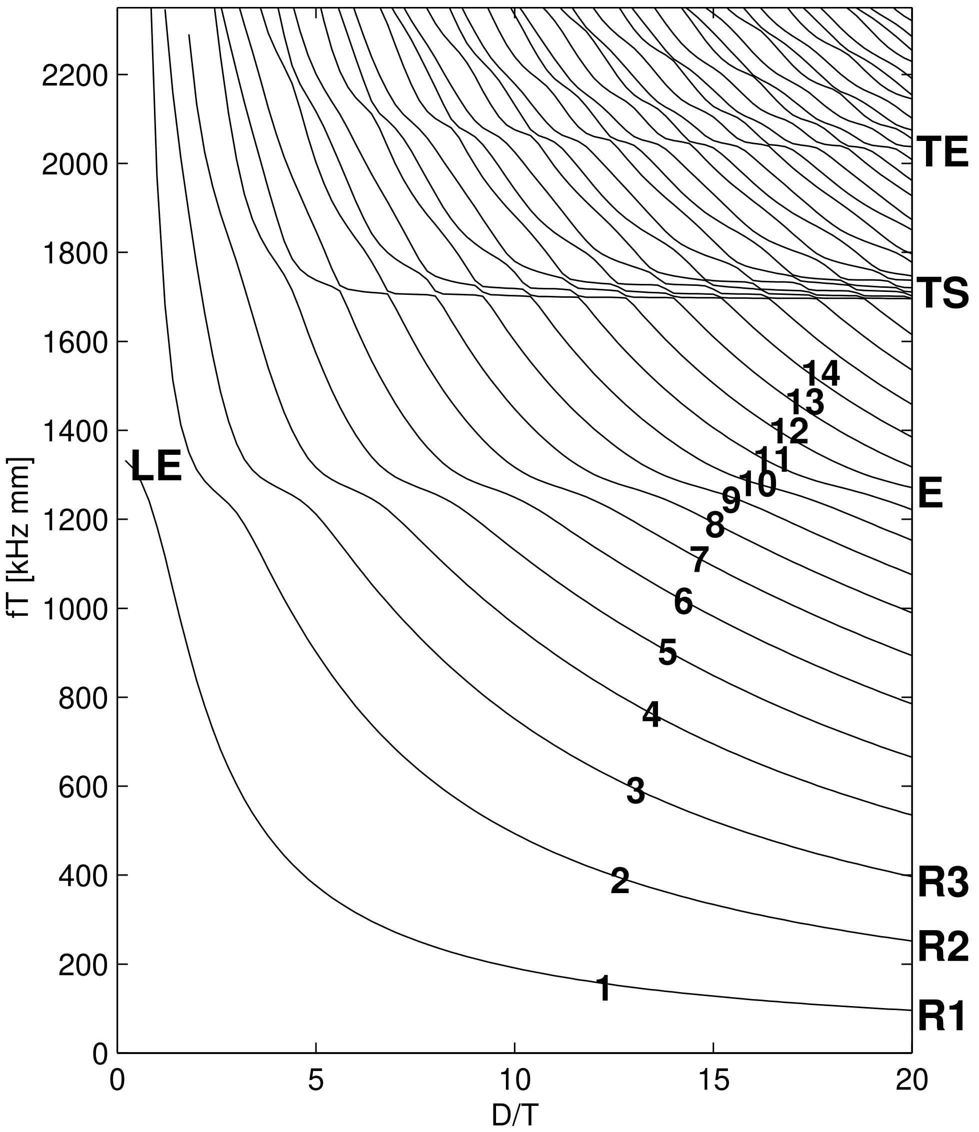

Figure 6. As Fig. 5, but for circular PZT-5H disks.

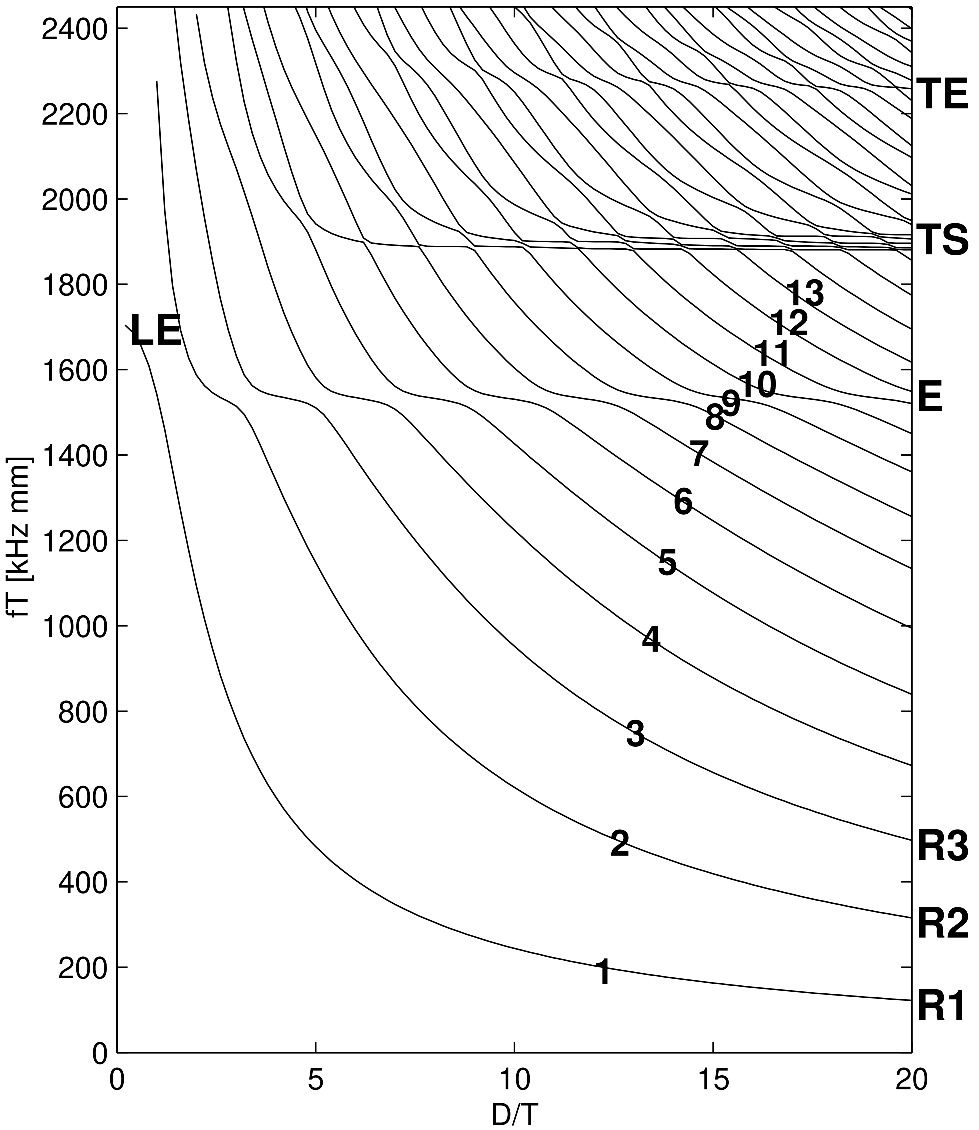

Figure 7. As Fig. 5, but for circular $Pb(ZrTi)O_3$ disks.

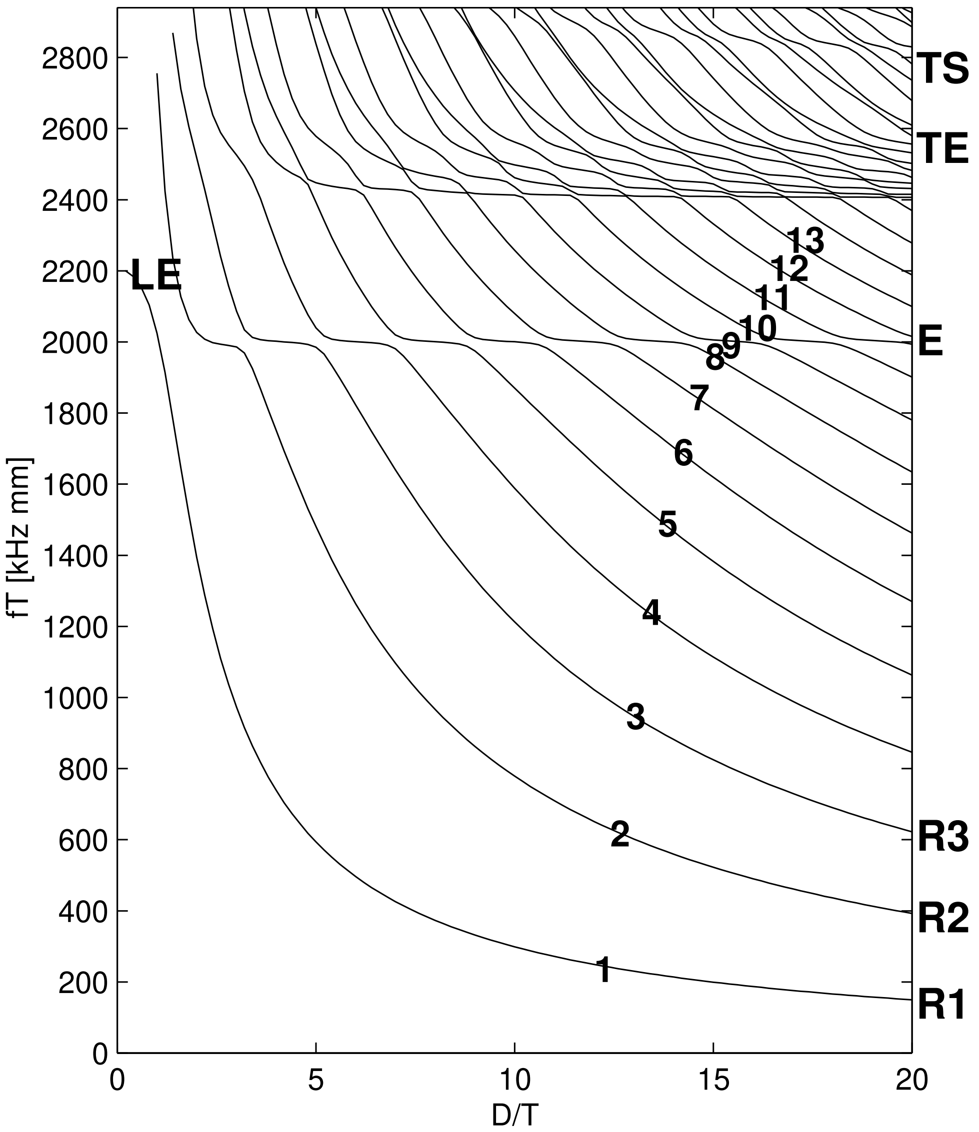

Figure 8. As Fig. 5, but for circular $BaTiO_3$ disks.

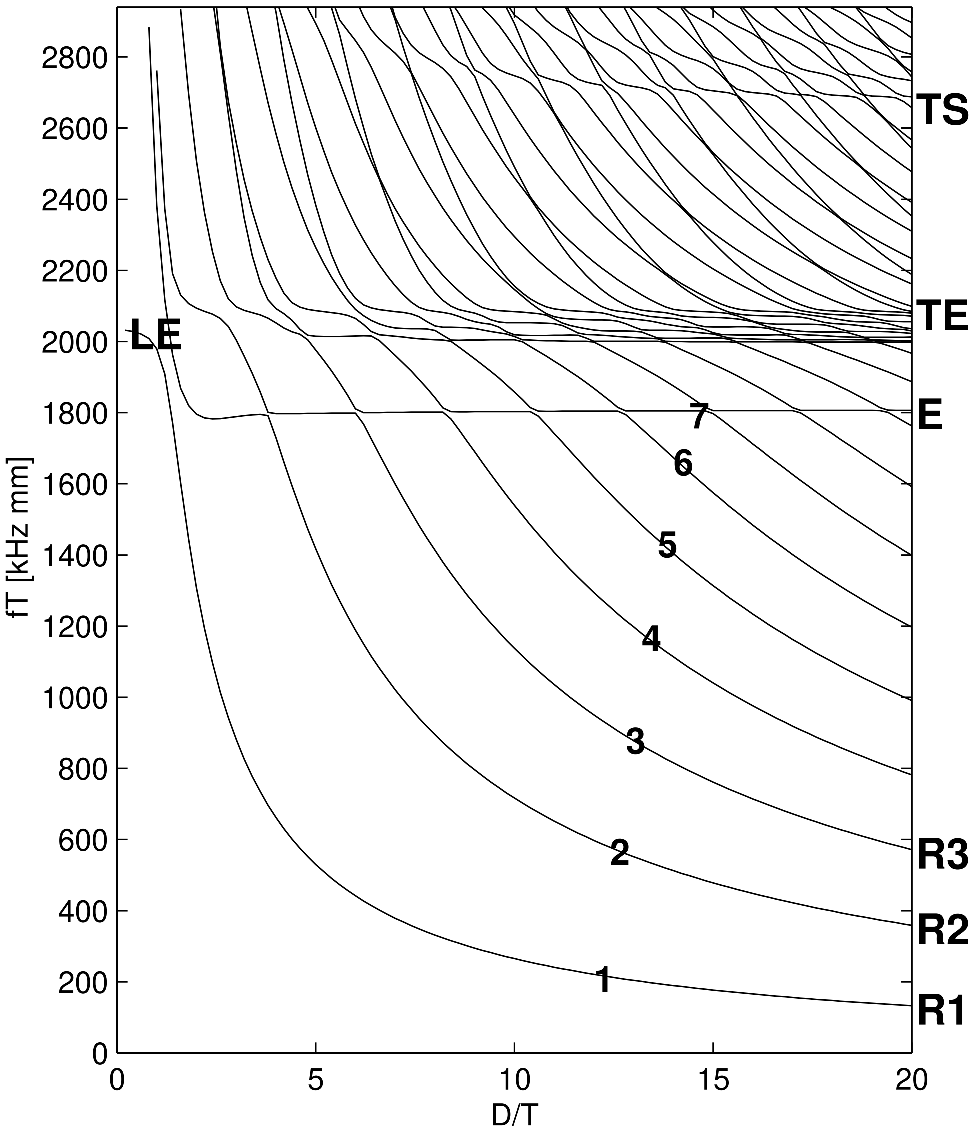

Figure 9. As Fig. 5, but for circular $PbTiO_3$ disks.

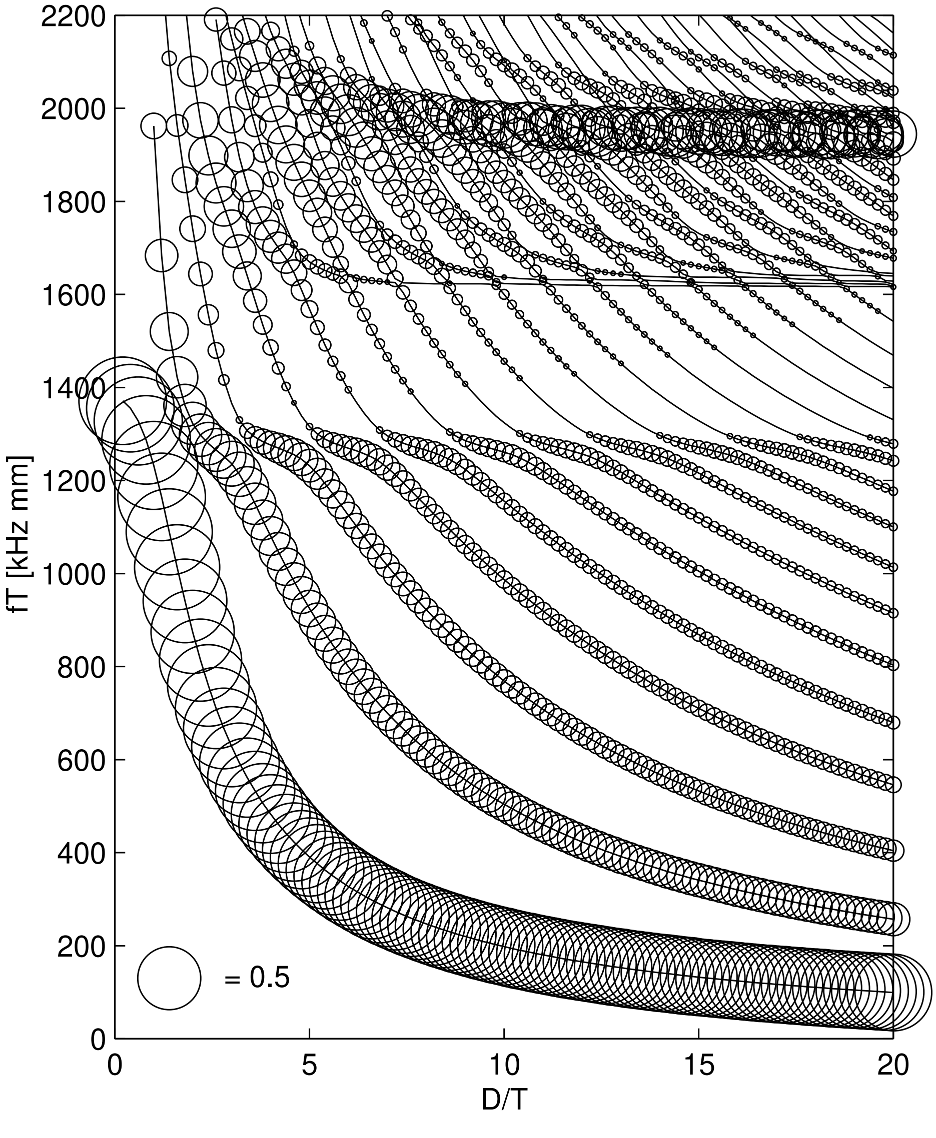

Figure 10. Resonance frequency spectrum for symmetric modes of circular PZT-5A disks. Circles proportional to k_{eff} are overlayed on the frequency spectrum for each resonance frequency.

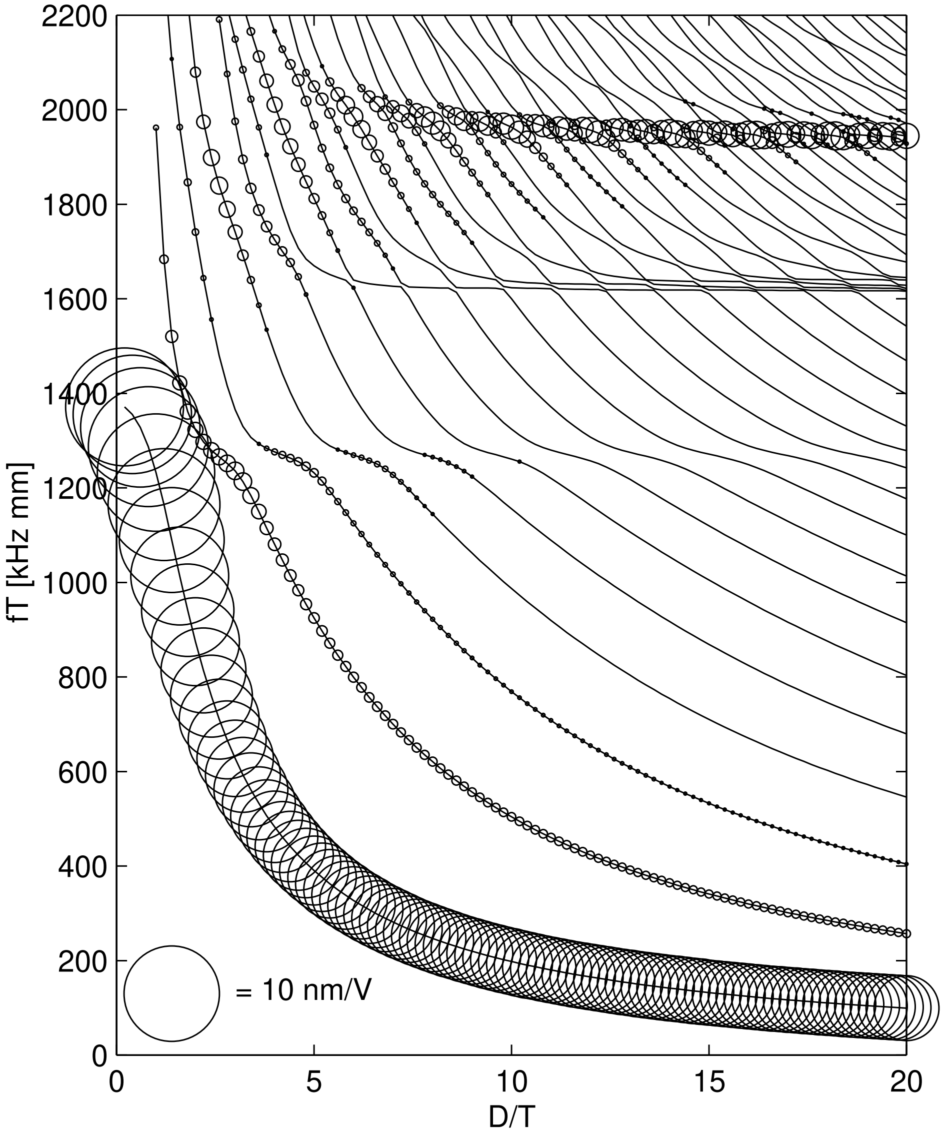

Figure 11. Resonance frequency spectrum for the symmetric modes of circular PZT-5A disks. Circles proportional to the average normal displacement per volt over the front of the disk are overlayed on the frequency spectrum for each resonance frequency.

Table I. The lowest 20 symmetric resonance frequencies of a PZT-5A disk with thickness 1.0 mm and diameter 10.0 mm calculated using FEMP and ABAQUS. For the simulations 35 elements are used in the radial direction and 7 elements in the thickness direction. Note that the results are identical to the decimals given by ABAQUS. The number of elements per shear wavelength used for each frequency is also given.

Mode number	FEMP [kHz]	ABAQUS [kHz]	Elements per shear wavelength
1	198.045	198.045	58.3
2	504.091	504.091	22.9
3	769.147	769.147	15.0
4	987.234	987.234	11.7
5	1155.74	1155.74	10.0
6	1260.99	1260.99	9.2
7	1324.15	1324.15	8.7
8	1456.57	1456.57	7.9
9	1600.01	1600.01	7.2
10	1623.17	1623.17	7.1
11	1636.95	1636.95	7.1
12	1707.46	1707.46	6.8
13	1749.68	1749.68	6.6
14	1842.80	1842.80	6.3
15	1908.50	1908.50	6.1
16	1963.02	1963.02	5.9
17	2006.89	2006.89	5.8
18	2092.74	2092.74	5.5
19	2103.21	2103.21	5.5
20	2181.01	2181.01	5.3

Table A1. Material parameters for the piezoelectric materials used in the convergence tests and resonance frequency spectra presented. $\epsilon_0 = 8.854 \times 10^{-12}$.

	PZT-5A	PZT-5H	$\mathrm{BaTiO_3}$	$\mathrm{Pb(ZrTi)O_3}$	$\mathrm{PbTiO_3}$
c_{11}^E $[10^{10} N/m^2]$	12.1	12.6	15.0	16.0939	14.3313
c_{12}^E $[10^{10} N/m^2]$	7.54	7.95	6.6	9.42719	3.22022
c_{13}^E $[10^{10} N/m^2]$	7.52	8.41	6.6	9.14505	2.41334
c_{33}^E $[10^{10} N/m^2]$	11.1	11.7	14.6	14.8873	13.1637
c_{44}^E $[10^{10} N/m^2]$	2.11	2.3	4.4	2.85714	5.58659
c_{66}^E $[10^{10} N/m^2]$	2.26	2.35	4.3	3.33333	5.55556
e_{11} $[C/m^2]$	−5.4	−6.5	−4.3	−1.48873	0.458534
e_{33} $[C/m^2]$	15.8	23.3	17.5	10.5997	6.50110
e_{15} $[C/m^2]$	12.3	17.0	11.4	10.5714	2.96089
$\epsilon_{11}^S/\epsilon_0$	916	1700	1115	480	210
$\epsilon_{33}^S/\epsilon_0$	830	1470	1260	270	140
ρ $[kg/m^3]$	7750	7500	5700	7700	7870

Table A2. Resonance frequencies of six PZT-5A disks with D/T ratio of 1.0, 4.0, 8.0, 12.0, 16.0 and 20.0. The thickness of all disks is 1.0 mm. The element division is given on the form $\mathrm{M_z x M_r}$ for each D/T ratio, where $\mathrm{M_z}$ is the number of elements in thickness direction and $\mathrm{M_r}$ is the number of elements in the radial direction.

Mode number	D/T= 1.0 14 x 7	D/T= 4.0 14 x 28	D/T= 8.0 14 x 56	D/T= 12.0 14 x 84	D/T= 16.0 14 x 112	D/T= 20.0 14 x 140
1	1232.370	482.810	246.911	165.271	124.126	99.365
2	1961.365	1080.739	620.757	423.366	319.922	256.809
3		1276.117	922.325	654.827	501.067	404.397
4		1485.498	1144.514	858.468	670.503	545.853
5		1724.332	1264.799	1027.167	824.346	679.522
6		1846.751	1350.043	1162.927	958.979	803.160
7		2009.690	1520.505	1256.889	1073.778	914.764
8		2164.993	1622.817	1307.457	1171.769	1013.467
9			1671.369	1413.758	1249.174	1100.176
10			1703.084	1532.137	1288.802	1176.982
11			1819.699	1619.199	1361.415	1242.185
12			1897.435	1630.405	1447.834	1278.892
13			1971.355	1651.236	1537.945	1330.724
14			2027.728	1659.174	1617.655	1398.128
15			2139.805	1735.947	1623.338	1468.708
16			2154.674	1780.226	1629.680	1541.426
17			2246.238	1857.648	1637.312	1615.146
18				1914.027	1647.884	1617.006
19				1956.467	1697.543	1621.077
20				1992.830	1725.235	1628.140
21				2054.709	1778.640	1639.204
22				2074.327	1820.482	1644.318
23				2133.766	1878.421	1677.451
24				2193.478	1922.249	1692.294
25				2247.177	1948.827	1733.791
26				2288.473	1978.574	1767.760
27					2011.625	1807.680
28					2040.952	1845.254
29					2074.835	1891.596
30					2111.850	1927.157
31					2169.231	1944.569
32					2181.085	1970.283
33					2223.378	1989.666
34					2293.362	2020.488
35						2037.569
36						2070.956
37						2113.427
38						2123.078
39						2159.499
40						2199.576
41						2227.195
42						2252.902
43						2291.138